# Understanding the color properties of $(C_5H_9NH_3)_2CuBr_4$ in high magnetic fields

J. D. Woodward, J. Choi, and J. L. Musfeldt
*Department of Chemistry, University of Tennessee, Knoxville, Tennessee 37996, USA*

J. T. Haraldsen
*Department of Physics, University of Tennessee, Knoxville, Tennessee 37996, USA*

X. Wei
*National High Magnetic Field Laboratory, Florida State University, Tallahassee, Florida 32306, USA*

H.-J. Koo, D. Dai, and M.-H. Whangbo
*Department of Chemistry, North Carolina State University, Raleigh, North Carolina 27695, USA*

C. P. Landee
*Department of Physics, Clark University, Worcester, Massachusetts 01610, USA*

M. M. Turnbull
*Carlson School of Chemistry and Biochemistry, Clark University, Worcester, Massachusetts 01610, USA*
(Received 28 April 2004; revised manuscript received 2 September 2004; published 20 May 2005)

We report the optical and magneto-optical properties of $(C_5H_9NH_3)_2CuBr_4$, an $S=1/2$ low-dimensional molecular antiferromagnet. Complementary electronic structure calculations demonstrate that the color properties of this material are dominated by excitations of the $CuBr_4^{2-}$ chromophore. In an applied magnetic field, $(C_5H_9NH_3)_2CuBr_4$ displays a rich magnetochromic response that is particularly strong in the direction of the bromide-bromide bridge pairs between the chains. This effect is attributed to a field-induced reorientation of the $CuBr_4^{2-}$ anions. These color changes are correlated with critical fields in the magnetization.

DOI: 10.1103/PhysRevB.71.174416 PACS number(s): 75.50.Ee, 71.20.−b, 78.20.Ls, 78.67.−n

## I. INTRODUCTION

Copper (II) halides are well known for their ability to adopt a diverse array of molecular and solid-state structures that provide good physical realizations of $S=1/2$ Heisenberg magnetic systems.[1] The remarkable structural diversity and flexibility of the copper-halide coordination sphere has produced a number of interesting low-dimensional magnetic systems including ladders, alternating chains, frustrated lattices, and two-dimensional layered structures.[2–14] Among the more important structural features are the single halide (Cu-*X*-Cu) and double halide (Cu-$X\cdots X$-Cu) bridges that mediate superexchange and super-superexchange interactions between the paramagnetic metal centers.[1,11,15–20] In general, the magnetic orbitals of copper halides are the frontier molecular orbitals comprised principally of Cu *d* and halide *p* atomic orbitals that are relatively close in energy. The effective spin exchange properties of the halide bridges stem from the significant electron delocalization from the metal orbitals to the ligand orbitals. While the single halide bridges can mediate both ferromagnetic and antiferromagnetic superexchange interactions, the double halide bridges typically mediate only antiferromagnetic exchange.[1,14,17,21–24] Furthermore, the magnitude of the exchange between double bromide bridges is typically larger than that between corresponding chloride bridges.[7,21,25–27] Major efforts have been directed toward understanding and tuning magnetostructural correlations in these systems.[1] Examples include layered $(RNH_3)_2CuX_4$ (where *R* is an organic cation and *X* is a halide) perovskitelike structures,[7,14–16,23–35] $Cu_2(C_5H_{12}N_2)_2Cl_4$ (abbreviated here as CuH-pCl),[36–42] and $(5IAP)_2CuBr_4\cdot 2H_2O$ (where 5-IAP is 5-iodo-2-aminopyridinium).[43]

One advantage of studying these materials, in particular those with double halide bridges, is that the coupling constants are often large enough in magnitude to be easily determined ($J/k\sim 5-15$ K) but small enough that the critical fields in the magnetization are relatively low ($H_c\leqslant 30$ T). In this case, the field dependent behavior can be conveniently investigated and the magnetization fully saturated with conventional superconducting or resistive magnet systems.[1,17,21,44] This is the case for CuHpCl and $(5IAP)_2CuBr_4\cdot 2H_2O$ as both display $H_c\sim 10$ T.[36–41,43] In contrast, other copper halides and oxides such as $TlCuCl_3$, $SrCu_2O_3$, and $CuGeO_3$, have very high critical fields, on the order of 100–300 T.[45–48] Macroscopic probes, such as resistivity, magnetization, and heat capacity, have traditionally been employed to investigate the bulk characteristics of materials in magnetic fields. Optical and magneto-optical spectroscopies are complementary and very sensitive tools for probing field-induced effects in low-dimensional magnetic solids as they allow correlation between bulk and microscopic properties.[49–62]

Bis(cyclopentylammonium)tetrabromocuprate, or $(CPA)_2CuBr_4$ ($CPA=C_5H_9NH_3$), is an example of a diammonium layered perovskite copper (II) halide system with both single halide-halide and double halide-halide bridges.[63]

 

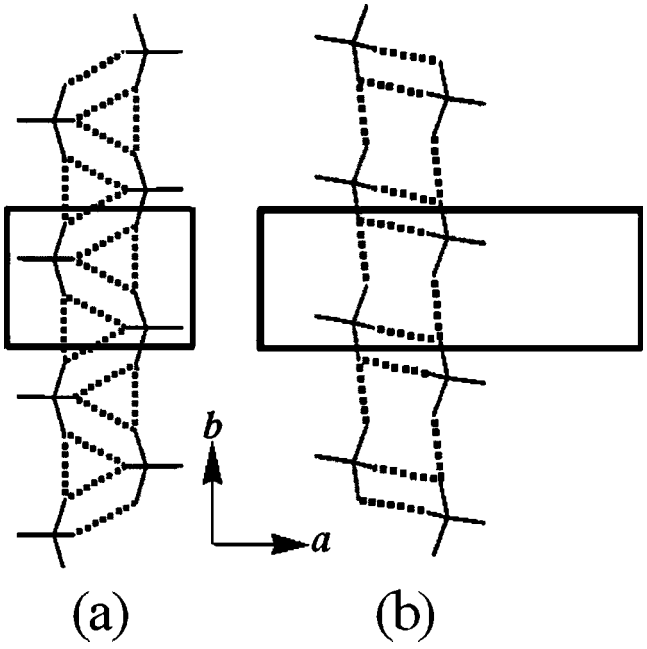


FIG. 1. The ladderlike molecular structure of $(CPA)_2CuBr_4$ in the *ab* plane at 300 K (a) and 200 K (b). For clarity, the organic cations are not shown.

As shown in Fig. 1, the double-chain, ladderlike structural arrangement of $CuBr_4^{2-}$ anions results from bromide-bromide bridges along the *b* axis (forming the chains) and pairs of bromide-bromide bridges between the chains (forming the rungs).[63] A structural phase transition involving reorientations of the CPA cation rings as well as slight displacements of the anions takes place at 260 K.[63] Based on the inequivalent bond lengths and angles in the $CuBr_4^{2-}$ anions (detailed structural information available in Ref. 63), $(CPA)_2CuBr_4$ has no *d* orbital degeneracy and is not a Jahn-Teller system. The low-temperature phase magnetic properties are consistent with those of an antiferromagnetic two-leg $S=1/2$ ladder system with two coupling constants $J_{rung}=-11.6$ K and $J_{leg}=-5.5$ K [Fig. 1(b)]. Within this picture, the high-temperature phase rung interactions cancel (by symmetry), and the magnetic lattice consists of isolated chains [Fig. 1(a)].[63] Independent of the detailed magnetic model, the magnitude of the coupling constants in $(CPA)_2CuBr_4$ is small enough that the critical fields [$H_{c1}\sim 2$ T (estimate) and $H_{c2}\sim 20$ T] are accessible by conventional powered magnet systems.[63] The magnetization saturates above $H_{c2}$. Despite the available magnetization data and the ladderlike character of the structure, $(CPA)_2CuBr_4$ should only be regarded as a spin-ladder *candidate*, pending inelastic neutron scattering experiments.[64,65] Spin dimer calculations also point out that the spin exchange pathways in a magnetic solid are not necessarily described by the topological arrangement of spin sites because magnetic orbitals are anisotropic.[66]

In order to provide additional information on the microscopic aspects of magnetically driven transitions in low-dimensional magnetic materials, we investigated the polarized optical and magneto-optical response of $(CPA)_2CuBr_4$. Complementary electronic structure calculations allow us to assign the main excitations of the $CuBr_4^{2-}$ chromophore. The field-induced changes in electronic structure are very rich, and we attribute the magnetochromic effect to chromophore reorientation in the magnetic field.

## II. METHODS

### A. Crystal growth and spectroscopy

Single crystals of $(CPA)_2CuBr_4$ were grown by evaporation of an aqueous solution containing a 2:1 ratio of $(C_5H_9NH_3)Br$ and $CuBr_2$. A few drops of HBr were added to the solution to avoid hydrolysis of the Cu(II) ions.[63] The blue-brown, platelike crystals have typical dimensions of $\sim 3\times 4\times 0.5$ mm$^3$. Crystallographic directions were determined by x-ray diffraction and carefully correlated with the optical response.

Near normal polarized reflectance measurements were carried out over a wide energy range (3.7 meV–6.2 eV; 30–50 000 cm$^{-1}$) using several different spectrometers including a Bruker 113 V Fourier transform infrared spectrometer, a Bruker Equinox 55 equipped with an infrared microscope, and a Perkin Elmer λ-900 instrument. The spectral resolution was 2 cm$^{-1}$ in the far and middle infrared and 2 nm in the near infrared, visible, and near ultraviolet. An aluminum mirror was used as the reference. Various wire grid, film, and crystal polarizers were employed, as appropriate. The optical axes of the crystal were determined as those that displayed the greatest anisotropy at 300 K and correspond to the *a* (mostly along the bromide-bromide bridge pairs) and *b* (primarily along the single bromide-bromide bridge) directions.[67] Low-temperature measurements were done with an open-flow cryostat equipped with a transfer line and temperature controller.[68] The optical conductivity was calculated from a Kramers-Kronig analysis of the measured reflectance, allowing us to extract information about dissipation in the material.[69,70]

The magneto-optical properties of $(CPA)_2CuBr_4$ were measured at the National High Magnetic Field Laboratory in Tallahassee, FL, using a grating spectrometer equipped with a CCD detector and a 30 T resistive magnet. The experiments were carried out in reflectance mode at 4.2 K. We concentrated on the *ab*-plane response; the field was applied perpendicular to the *ab* plane of the crystal. The measurements covered the energy range from 1.1–3.5 eV (350–1100 nm). A series of Polaroid film polarizers were used to obtain the desired directional selectivity. The field-induced changes in the polarized optical reflectance spectra of $(CPA)_2CuBr_4$ are best visualized by calculating reflectance ratios. This rendering presents a normalized response, which gives good sensitivity to field-induced color changes. For example, the 1 T/0 T reflectance ratio gives the minimum field-induced effect and the 30 T/0 T yields the maximum magneto-optical signature at 4.2 K. We quantified the field-induced spectral changes with standard peakfitting techniques. Inflection points in the integrated area versus field curves are used to identify phase boundaries in *H-T* space.[56]

### B. Electronic structure calculations

To estimate the allowed electronic transitions and their excitation energies of the $CuBr_4^{2-}$ anion in $(CPA)_2CuBr_4$, we

carried out spin-polarized density functional theory (DFT) electronic structure calculations for the idealized structure of the $CuBr_4^{2-}$ anion [$C_{2v}$ symmetry; Cu-Br(1)=2.358 Å, Cu-Br(2)=2.363 Å, Br(1)-Cu-Br(1)=125.66°, Br(2)-Cu-Br(2)=134.13°] based on the room-temperature crystal structure of $(CPA)_2CuBr_4$ using the GAUSSIAN 98 program package.[71] The 6-31$G(d)$ basis sets and B3LYP functional[72] were employed in the unrestricted calculations, and the $^2B_2$ state was obtained as the ground state. The DFT calculations show that 75% of the unpaired spin density resides on the Cu(II) ion and that 25% is distributed evenly over the $Br^-$ ions. We then performed extended Huckel tight binding (EHTB) calculations[73] by adjusting the valence state ionization potential of Br until this DFT result was reproduced. Then we employed EHTB calculations to analyze the symmetries, the orbital shapes, and the molecular orbital energies of $CuBr_4^{2-}$.

## III. RESULTS AND DISCUSSION

### A. Optical properties and electronic structure calculations of $(CPA)_2CuBr_4$

Figure 2 displays the variable temperature reflectance and optical conductivity of $(CPA)_2CuBr_4$ along the *a* direction, which is primarily along the double bromide-bromide bridges that form the rungs of the structural ladder. Only modest differences were observed between the *a* and *b* polarizations, so the *b*-directed spectra are not presented here.[74–76] The optical spectrum of $(CPA)_2CuBr_4$ displays a number of electronic excitations similar to those in other low-dimensional copper halides.[77,78] Detailed assignments are given below.

Electronic structure calculations were used to determine the allowed excitations in $(CPA)_2CuBr_4$. The 17 highest occupied molecular orbitals of $CuBr_4^{2-}$ consist principally of 12 *p*-block levels from the four $Br^-$ ions and 5 *d*-block levels from the Cu(II) ion. The symmetries of these orbitals are classified within the $C_{2v}$ point group. For the purposes of these calculations, the $CuBr_4^{2-}$ ion was placed in a coordinate system where the *x* axis is along the Br(1)···Br(1) direction which runs parallel to the chains of the structural ladder, the *y* axis is along the Br(2)···Br(2) direction which runs parallel to the rungs of the structural ladder, and the *z* axis lies along the twofold rotation axis of the $CuBr_4^{2-}$ ion, perpendicular to the large crystal face. According to this coordinate system, orbital symmetries are grouped as 6 $A_1$, 4 $B_1$, 4 $B_2$, and 3 $A_2$. The low-lying orbitals are doubly occupied. The highest occupied molecular orbital is singly occupied and has $A_1$ symmetry. Electronic excitations are predicted to occur from the doubly occupied molecular orbitals to the highest (singly) occupied molecular orbital of $A_1$ symmetry. The allowed transitions can be obtained by considering the change in dipole selection rules. A pictorial summary of the allowed intramolecular optical excitations in the $CuBr_4^{2-}$ chromophore and their associated energies are shown in Fig. 3.

From these calculations, the most well-defined features in the *a* polarized optical conductivity spectrum of $(CPA)_2CuBr_4$ [Fig. 2(b)] can be assigned. The weak low-energy peak at ~0.79 eV is assigned to the $4B_2$ to $6A_1$ excitation, and the triplet at ~1.91, 2.13, and 2.34 eV is assigned to the $3B_2$ to $6A_1$, $2B_2$ to $6A_1$ and $1B_2$ to $6A_1$ excitations, respectively. The peaks at ~3.5 eV and above are related to excitations from filled *s* orbitals to the highest occupied molecular orbital and/or charge transfer between the organic cation and the $CuBr_4^{2-}$ anion. These higher energy transitions were not considered in the model calculations.

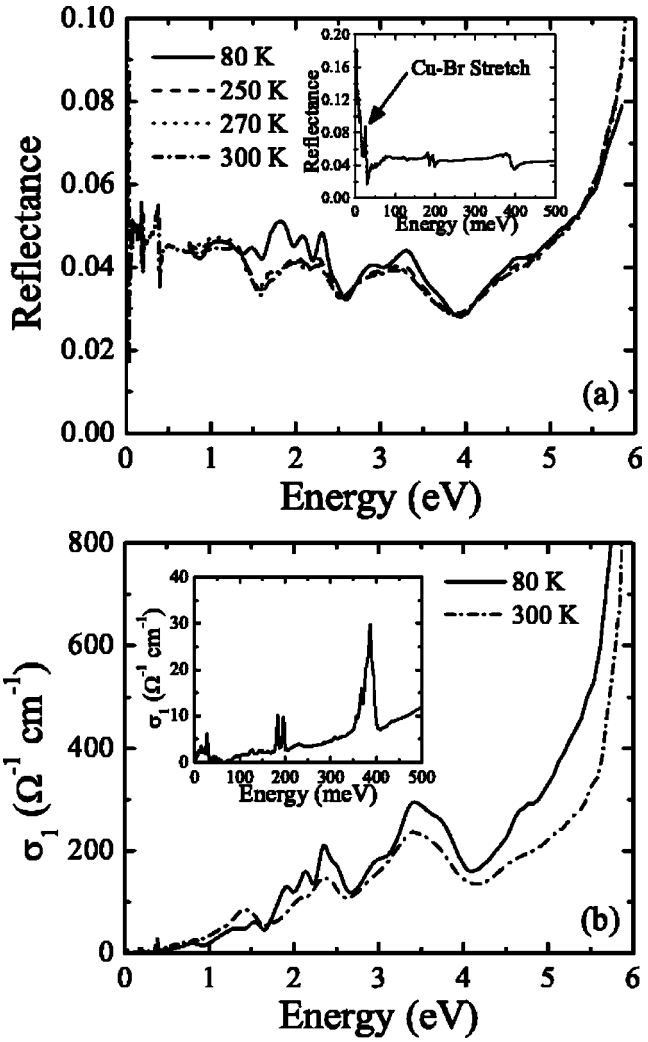


FIG. 2. Variable temperature reflectance (a) and optical conductivity (b) of $(CPA)_2CuBr_4$ along the *a* direction, corresponding to the response mainly along the double bromide-bromide bridge pairs. Data were collected at 80 K (solid line), 250 K (dashed line), 270 K (dotted line), and 300 K (dotted-dashed line). The insets in both figures focus on the phonon modes of $(CPA)_2CuBr_4$ at 300 K.

### B. Magneto-optical properties of $(CPA)_2CuBr_4$

Figure 4(a) shows the magneto-optical properties of $(CPA)_2CuBr_4$ along the *a* direction, which is mostly along the bromide-bromide bridge pairs. Application of a magnetic field redistributes the spectral weight related to the intramolecular chromophore excitations, and these changes are seen as a series of peaks and dips in the normalized reflectance ratio data. The largest field-induced change in the color prop-

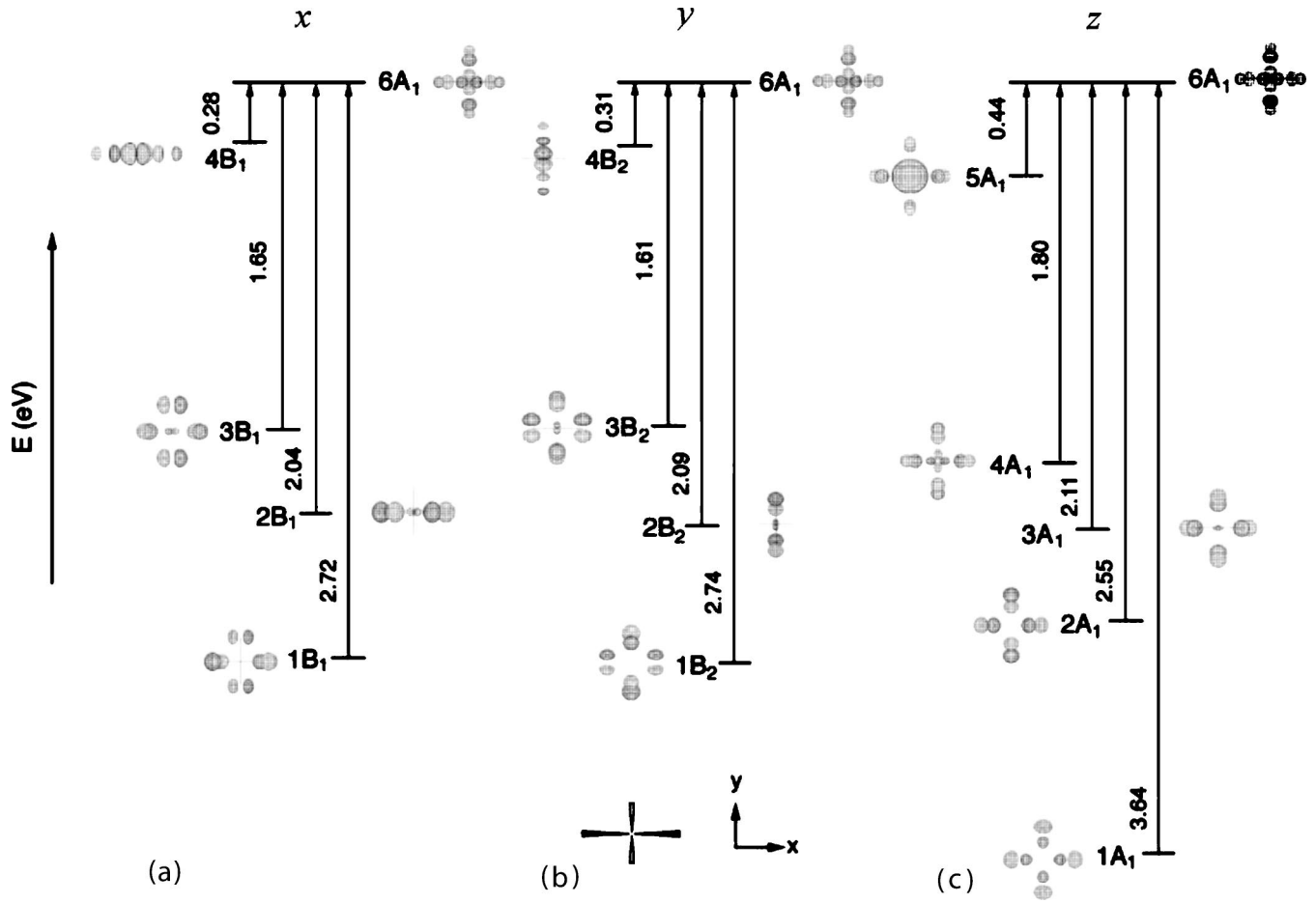


FIG. 3. Predicted optical excitations from filled *p*- and *d*-block energy levels to the singly occupied $6A_1$ level of the $CuBr_4^{2-}$ chromophore along the (a) *b* axis, (b) *a* axis, and (c) *c* axis, corresponding to the directions of *x*, *y*, and *z*, respectively. Predicted excitations energies (in eV) are shown. Relevant orbitals in the $CuBr_4$ chromophore are also diagrammed.

erties of $(CPA)_2CuBr_4$ is centered at about 2.75 eV, where the reflectance increases by $>7\%$ in a 30 T field. Between $\sim$2.0 and 2.6 eV, reflectance decreases by about 2% under the same conditions. Several smaller changes are observed below 2 eV. We refer to the magnetic field-induced color change in $(CPA)_2CuBr_4$ as "magnetochromism." Field-induced optical effects have also been observed in other transition metal halides.[53,54]

Figure 4(b) shows the integrated area of the 2.75 eV peak and the features between 2.00 and 2.6 eV as a function of applied magnetic field. Careful examination of the integrated area vs field plot shows small inflection points in the response. We used both numerical derivatives and visual inspection to determine slope changes. The inflection points are indicated in Fig. 4(b) as dashed vertical lines at $\sim$7, 13, 18, and 23.5 T. As discussed below, these field-induced color changes seem to correlate with changes in the bulk magnetic properties. The magneto-optical effect is nearly saturated at 30 T, consistent with the magnetization.[63]

Figure 5(a) displays the magneto-optical reflectance ratio spectra of $(CPA)_2CuBr_4$ along *b*, the direction of the single bromide-bromide bridges. A modest field-induced color change is observed ($\sim$2% at 30 T). Although the absolute optical conductivity of $(CPA)_2CuBr_4$ is nearly isotropic, the magneto-optical spectra are highly anisotropic. As an example, the $\sim$2.75 eV excitation is very strong along the *a* direction [Fig. 4(a)], but completely absent in the *b* direction [Fig. 5(a)]. This anisotropy and the relative size of the magneto-optical effect provides important clues to the mechanism of the field-induced color change in $(CPA)_2CuBr_4$, as discussed below.

Figure 5(b) shows the integrated area of several features in the *b*-polarized reflectance ratio spectra as a function of applied magnetic field. Structures at 1.60 and 2.00 eV grow modestly above 5 T and saturate by 20 T. In contrast, the 1.25 and 1.80 eV features grow rapidly above 10 T and show no sign of saturation, even at $H=30$ T. Inflection points in the magneto-optical response are observed at $\sim$6, 13, 17.5, and 24 T; they are indicated by vertical dashed lines in Fig. 5(b). Within our sensitivity, the critical fields in both polarizations are identical. Table I summarizes the critical fields and the important electronic excitations.

Interestingly, magnetochromism in $(CPA)_2CuBr_4$ is correlated with the bulk magnetic behavior. Figure 6 shows the field-dependent magnetization measured at 0.74 K along with the corresponding derivative with respect to field.[63] Four inflection points are identified in this data. The first (estimated to be near $\sim$2 T) and the last (at $\sim$20 T) have

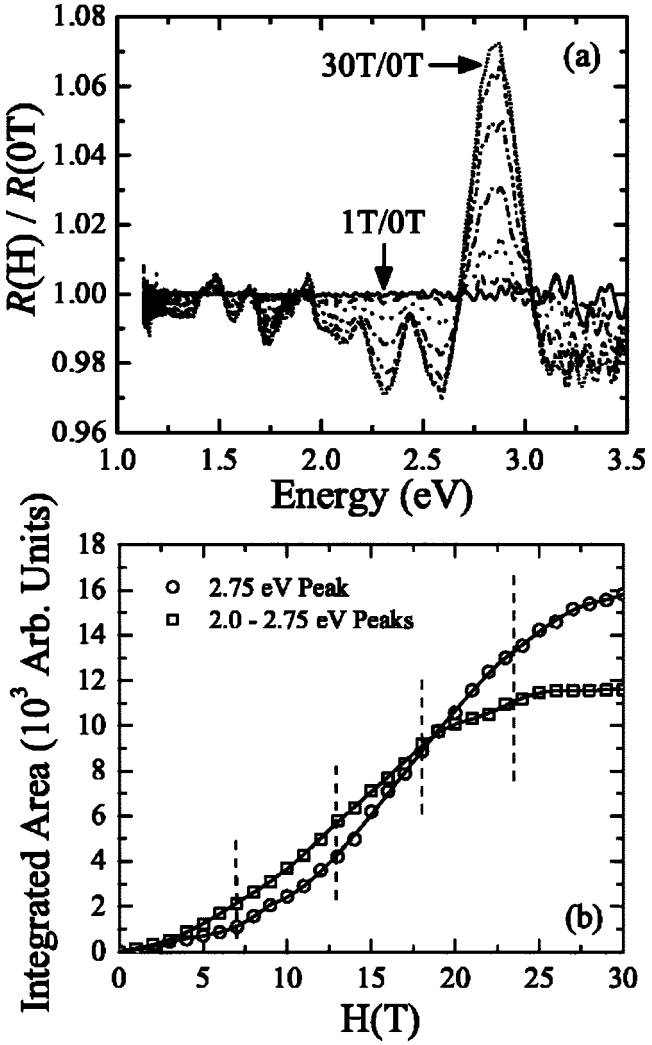


FIG. 4. The normalized magneto-optical response $R(H)/R(0\mathrm{T})$, (a) of $(CPA)_2CuBr_4$ along the *a* direction (bromide-bromide bridge pairs) at 4.2 K. The field-dependent integrated area (b) of the features between 2.00–2.6 eV (square) and that centered at 2.75 eV (circle). Changes in slope and inflection points in the data are denoted by vertical dashed lines.

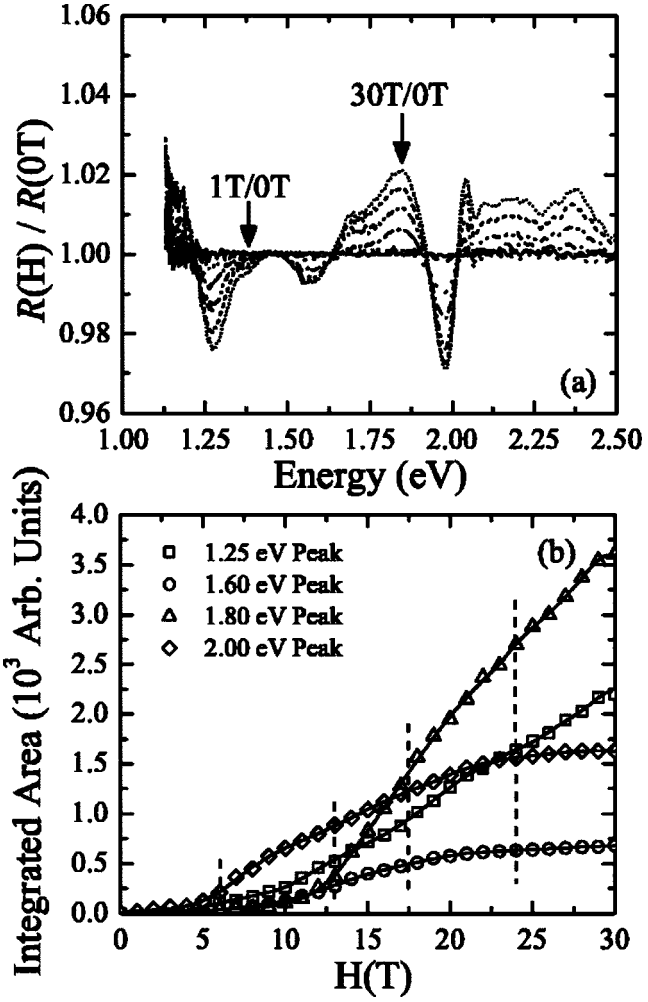


FIG. 5. The normalized magneto-optical response $R(H)/R(0\mathrm{T})$, (a) of $(CPA)_2CuBr_4$ along the single bromide-bromide chains (*b* direction) at 4.2 K. For viewing purposes, the energy axis is smaller than that in Fig. 4. The field-dependent integrated area (b) of the features centered at 1.25 eV (square), 1.60 eV (circle), 1.80 eV (triangle), and 2.00 eV (diamond). Changes in slope and inflection points in the data are denoted by vertical dashed lines.

been assigned as the lower ($H_{c1}$) and upper ($H_{c2}$) critical fields, respectively.[63,79] Critical fields from high-field spectroscopic data compare reasonably well with those from the bulk magnetization. The 7 and 24 T fields from the magneto-optical measurements are assigned as $H_{c1}$ and $H_{c2}$, respectively. This assignment is based upon the observation that critical fields from the magnetization of $(CPA)_2CuBr_4$ and related materials increase with increasing measurement temperature and broaden as well.[46,63] The two additional magnetically driven transitions observed in the spectroscopic data (at 13 and 17 T) may be related to the weak features in the bulk magnetization at ~7 and 12 T. It is interesting that similar transitions, intermediate between $H_{c1}$ and $H_{c2}$, have been observed in $KCuCl_3$, $TlCuCl_3$, and CuHpCl, but have not been addressed at either the bulk or microscopic level.[36–42,45,46]

We considered several scenarios to explain the various aspects of the field-induced color change in $(CPA)_2CuBr_4$. These include (1) magnetic coupling theories, (2) field-induced bulk strain, and (3) field-induced reorientation of chromophore units. Each is discussed below, although we

TABLE I. Summary of critical fields in $(CPA)_2CuBr_4$ as determined from the magneto-optical properties, the relationship to the critical fields extracted from bulk magnetization, and the electronic excitations involved in each field-driven transition.

| Transition field (T) | Assignment | Chain excitations (eV) | Rung excitations (eV) |
|---|---|---|---|
| 6–7 | $H_{c1}$ | 1.25, 1.60, 2.00 | 2.0–2.6, 2.75 |
| 13 | See text | 1.25, 1.60, 2.00 | 2.0–2.6, 2.75 |
| 17 | See text | 1.25, 1.60, 1.80, 2.00 | 2.0–2.6, 2.75 |
| 24 | $H_{c2}$ | 1.25, 1.80 | 2.0–2.6, 2.75 |

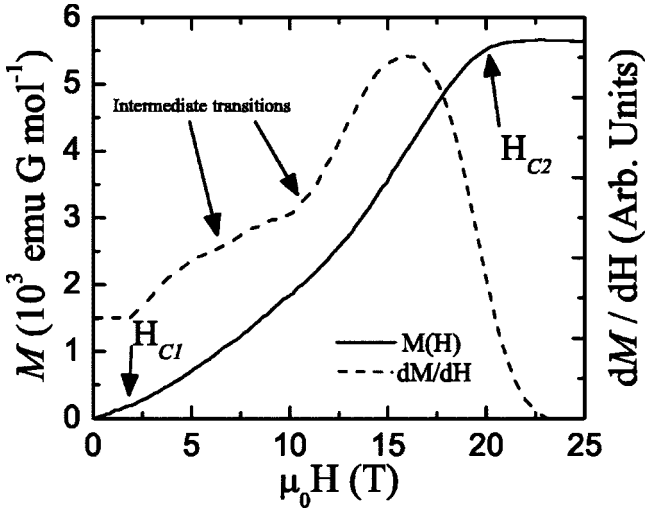


FIG. 6. The field-dependent molar magnetization $M$ of $(CPA)_2CuBr_4$ (solid line) and derivative of the magnetization with respect to the field $dM/dH$ (dashed line) at 0.74 K (Ref. 63). Magnetization shows a clear change at 20 T and an estimated change near 2 T (due to thermal occupation of the excited states that smear the magnetization) that are assigned as upper and lower critical fields, respectively. The magnetization saturates above $H_{c2}$ (Ref. 63). Nacent features are also found at intermediate fields. The latter appear as inflection points in the $dM/dH$ data.

regard the third as most promising, mainly due to energy scale arguments.

(1) Theoretical models for two-leg spin ladders do not predict plateaus between $H_{c1}$ and $H_{c2}$.[80–83] The presence of intermediate field transitions suggests that $(CPA)_2CuBr_4$ does not behave as a simple two-leg spin ladder and that additional interactions or frustrations may be present. In such a case, more complex magnetic coupling theories should be employed.[80–83] Interladder hydrogen bonding through the organic cations and other interchain Br···Br contacts may provide pathways for additional superexchange interactions. Inelastic neutron scattering can quantify these effects.

(2) The second mechanism considered by us to account for the observed magneto-optical effect and intermediate field transitions in $(CPA)_2CuBr_4$ involves field-induced bulk distortions of the unit cell to relieve stress. Such a mechanism was recently discussed for CrN, where magnetic stress is the driving force of structural distortion.[84] However, given the energy scale of such a bulk modification and the molecular nature of the title compound, this type of bulk distortion seems unlikely.

(3) The most plausible scenario to explain the observed magnetochromic effect in $(CPA)_2CuBr_4$ and the inflection points in that response involves field-induced reorientations of the chromophore. This mechanism differs from large-scale distortions of the crystal as a whole in that the barriers to $CuBr_4^{2-}$ anion rotation with respect to one another are small, due to the weak Br···Br contacts, and a number of different rotational positions of the chromophore are possible. This picture is essentially an extension of (2), modified to allow a field-induced change in local structure that is appropriate for a molecular compound. Cooperative rotations and "paddle wheel" mechanisms have been identified in other molecular solids.[85,86]

We propose that the chromophore rotates about the chain direction of the low-dimensional structure with applied field because the principal components of the $g$-tensor of the spin Hamiltonian encourage the $CuBr_4^{2-}$ anions to align with the field. The pivoting about the chains upsets the double Br···Br bridge contacts along the rungs of the ladderlike structure and gives rise to small changes in the local $CuBr_4^{2-}$ environment. This rotation also modifies the direction of the dipole moment operator, and is manifested as a change in the optical properties with field. Plateaus in the magneto-optical response at intermediate fields may correspond to locally favorable positions of the chromophore.

Both the molecular structure of $(CPA)_2CuBr_4$ and the low-energy scale of the proposed chromophore rotations support this mechanism. The $CuBr_4^{2-}$ anions are loosely bound to one another in the molecular solid through relatively weak halide-halide contacts. The single Br···Br contacts may render movement and reorientation of the $CuBr_4^{2-}$ anions about the chains easier than along the double Br···Br bridge pairs. This difference may account for the anisotropic magneto-optical properties of $(CPA)_2CuBr_4$. The proposed field-induced reorientation of the $CuBr_4^{2-}$ anions is also in line with energy scale arguments, since the relevant energy scale in $(CPA)_2CuBr_4$ is considerably smaller than that required to distort an entire crystal or cause atoms to move in a covalently bound solid. Using the well-known relationship between temperature and magnetic field (1.4 K $\sim$ 1 T for $g=2$), we conclude that $(CPA)_2CuBr_4$ is very plastic and is deformable at the rather small energy of 30 T (or $\sim$45 K). There is no hysteresis in the magneto-optical response, which implies that the local field-induced structural deformations are reversible, consistent with the chromophore rotation mechanism.

## IV. CONCLUSION

The optical and magneto-optical properties of $(CPA)_2CuBr_4$, an $S=1/2$ molecular antiferromagnet, have been investigated in order to understand the interplay between the spin, lattice, charge, and orbital degrees of freedom in this novel copper halide. Complementary electronic structure calculations demonstrate that the color properties of this low-dimensional material are dominated by the excitations of the $CuBr_4^{2-}$ chromophore. In an applied magnetic field, $(CPA)_2CuBr_4$ displays a rich and unusually anisotropic magneto-optical response; it is very strong in the direction of the bromide-bromide bridge pairs, more than 7% at 30 T. This effect is attributed to a field-induced reorientation of the $CuBr_4^{2-}$ anions about the chains within the solid. It is particularly interesting that the proposed chromophore rotations do not take place gradually, but instead seem to require critical fields for their displacement. These color changes are correlated with critical fields from the magnetization. Similar features seem to appear in the magnetization of other low-dimensional magnetic materials and may be a consequence of field-induced local structural modifications.

**ACKNOWLEDGMENTS**

This project was supported by the Materials Science Division, Basic Energy Sciences at the U.S. Department of Energy at the University of Tennessee (DE-FG02-01ER45885) and North Carolina State University (DE-FG02-86ER45259), and also by the Division of Materials Research at the National Science Foundation (DMR-9803813) at Clark University. A portion of this work was performed at the National High Magnetic Field Laboratory, which is supported by NSF Cooperation Agreement DMR-0084173 and by the State of Florida. Useful conversations with R. D. Willett, as well as the x-ray diffraction work of C. Nygren, and selected polarization measurements of R. Wesolowski are gratefully acknowledged.

[1] *Magneto-Structural Correlations in Exchange Coupled Systems*, edited by R. D. Willett, D. Gatteschi, and O. Kahn, Vol. 140 of *NATO ASI Series C: Mathematical & Physical Sciences* (Reidel, Dordrecht, 1985).
[2] S. F. Haddad, R. D. Willett, and C. P. Landee, Inorg. Chim. Acta **316**, 94 (2001).
[3] R. D. Willett, Mol. Cryst. Liq. Cryst. Sci. Technol., Sect. A **273**, A71 (1995).
[4] T. E. Grigereit, Y. Liu, P. Zhou, J. E. Drumheller, A. Bonomartini-Corradi, M. R. Bond, H. Place, and R. D. Willett, J. Magn. Magn. Mater. **104**, 831 (1992).
[5] M. R. Bond, R. D. Willett, and G. V. Rubenacker, Inorg. Chem. **29**, 2713 (1990).
[6] C. P. Landee, A. Djili, D. F. Mudgett, M. Newhall, H. Place, B. Scott, and R. D. Willett, Inorg. Chem. **27**, 620 (1988).
[7] R. D. Willett, H. Place, and M. Middleton, J. Am. Chem. Soc. **110**, 8639 (1988).
[8] P. Zhou, J. E. Drumheller, G. V. Rubenacker, M. R. Bond, and R. D. Willett, J. Phys. (Paris) **49**, C8, 1471 (1988).
[9] C. E. Zaspel, G. V. Rubenacker, S. L. Hutton, J. E. Drumheller, R. S. Rubins, R. D. Willett, and M. R. Bond, J. Appl. Phys. **63**, 3028 (1988).
[10] B. Scott and R. D. Willett, J. Appl. Phys. **61**, 3289 (1987).
[11] U. Geiser, R. M. Gaura, R. D. Willett, and D. X. West, Inorg. Chem. **25**, 4203 (1986).
[12] R. D. Willett, R. J. Wong, and M. Numata, Inorg. Chem. **22**, 3189 (1983).
[13] H. A. Groenendijk, H. W. J. Blöte, A. J. van Duyneveldt, R. M. Gaura, C. P. Landee, and R. D. Willett, Physica A **106**, 47 (1981); R. Hoogerbeets, S. A. J. Weigers, A. J. van Duyneveldt, R. D. Willett, and U. Geiser, *ibid.* **125**, 135 (1984).
[14] L. O. Snively, P. L. Seifert, K. Emerson, and J. E. Drumheller, Phys. Rev. B **20**, 2101 (1979).
[15] G. S. Long, M. Wei, and R. D. Willett, Inorg. Chem. **36**, 3102 (1997).
[16] N. Sivron, T. E. Grigereit, J. E. Drumheller, K. Emerson, and R. D. Willett, J. Appl. Phys. **75**, 5952 (1994).
[17] P. Zhou, J. E. Drumheller, G. V. Rubenacker, K. Halvorson, and R. D. Willett, J. Appl. Phys. **69**, 5804 (1991).
[18] C. P. Landee and R. D. Willett, Phys. Rev. Lett. **43**, 463 (1979).
[19] D. D. Swank, C. P. Landee, and R. D. Willett, Phys. Rev. B **20**, 2154 (1979).
[20] D. D. Swank, C. P. Landee, and R. D. Willett, J. Magn. Magn. Mater. **15-18**, 319 (1980).
[21] C. Chow and R. D. Willett, J. Chem. Phys. **59**, 5903 (1973).
[22] T. E. Grigereit, J. E. Drumheller, B. Scott, G. Pon, and R. D. Willett, J. Magn. Magn. Mater. **104**, 1981 (1992).
[23] G. V. Rubenacker, S. Waplak, S. L. Hutton, D. N. Haines, and J. E. Drumheller, J. Appl. Phys. **57**, 3341 (1985).
[24] L. O. Snively, G. F. Tuthill, and J. E. Drumheller, Phys. Rev. B **24**, 5349 (1981).
[25] C. P. Landee, K. Halvorson, and R. D. Willett, J. Appl. Phys. **61**, 3295 (1987).
[26] P. Straatman, R. Block, and L. Jansen, Phys. Rev. B **29**, 1415 (1984).
[27] R. Block and L. Jansen, Phys. Rev. B **26**, 148 (1982).
[28] R. D. Willett, Acta Crystallogr., Sect. C: Cryst. Struct. Commun. **46**, 565 (1990).
[29] K. Halvorson and R. D. Willett, Acta Crystallogr., Sect. C: Cryst. Struct. Commun. **44**, 2071 (1988).
[30] R. D. Willett, H. Place, and M. Middleton, J. Am. Chem. Soc. **110**, 8639 (1988).
[31] L. O. Snively, D. N. Haines, K. Emerson, and J. E. Drumheller, Phys. Rev. B **26**, 5245 (1982).
[32] K. Tichy, J. Benes, W. Halg, and H. Arend, Acta Crystallogr., Sect. B: Struct. Crystallogr. Cryst. Chem. **34**, 2970 (1978).
[33] L. J. De Jongh and A. R. Miedema, Adv. Phys. **23**, 1 (1974).
[34] F. Barendregt and H. Schenk, Physica (Amsterdam) **49**, 465 (1970).
[35] J. P. Steadman and R. D. Willett, Inorg. Chim. Acta **4**, 367 (1970).
[36] Q. Gu, D.-K. Yu, and J.-L. Shen, Phys. Rev. B **60**, 3009 (1999).
[37] P. R. Hammar, D. H. Reich, C. Broholm, and F. Trouw, Phys. Rev. B **57**, 7846 (1998).
[38] G. Chaboussant, P. A. Crowell, L. P. Levy, O. Piovesana, A. Madouri, and D. Mailly, Phys. Rev. B **55**, 3046 (1997).
[39] G. Chaboussant, M. H. Julien, Y. Fagot-Revurat, L. P. Levy, C. Berthier, M. Horvatić, and O. Piovesana, Phys. Rev. Lett. **79**, 925 (1997).
[40] Zheng Weihong, R. R. P. Singh, and J. Oitmaa, Phys. Rev. B **55**, 8052 (1997).
[41] C. A. Hayward, D. Poilblanc, and L. P. Levy, Phys. Rev. B **54**, R12 649 (1996).
[42] B. Chiari, O. Piovesana, T. Tarantelli, and P. F. Zanazzi, Inorg. Chem. **28**, 2141 (1989).
[43] C. P. Landee, M. M. Turnbull, C. Galeriu, J. Giantsidis, and F. M. Woodward, Phys. Rev. B **63**, 100402(R) (2001).
[44] B. R. Patyal, B. L. Scott, and R. D. Willett, Phys. Rev. B **41**, 1657 (1990).
[45] H. Tanaka, W. Shiramura, T. Takatsu, B. Kurniawan, M. Takahashi, K. Takizawa, H. Mitamura, and T. Goto, Physica B **246**, 230 (1998).
[46] W. Shiramura, K. Takatsu, H. Tanaka, K. Kamishima, M. Takahashi, H. Mitamura, and T. Goto, J. Phys. Soc. Jpn. **66**, 1900 (1997).
[47] H. Nojiri, Y. Shimamoto, N. Miura, M. Hase, K. Uchinokura, H.

Kojima, I. Tanaka, and Y. Shibuya, Phys. Rev. B **52**, 12 749 (1995).
[48] M. Azuma, Z. Hiroi, M. Takano, K. Ishida, and Y. Kitaoka, Phys. Rev. Lett. **73**, 3463 (1994).
[49] K. Kakurai, M. Nishi, K. Nakajima, T. Yoshihama, M. Isobe, Y. Ueda, T. Kato, H. Tanaka, A. Hoser, and H. A. Graf, J. Phys. Soc. Jpn. **69**, 78 (2000).
[50] T. Masui, M. Limonov, H. Uchiyama, S. Lee, S. Tajima, and A. Yamanaka, Phys. Rev. B **68**, 060506(R) (2003).
[51] S. Uchida, T. Ido, H. Takagi, T. Arima, Y. Tokura, and S. Tajima, Phys. Rev. B **43**, 7942 (1991).
[52] S. W. Moore, J. M. Graybeal, D. B. Tanner, J. Sarrao, and Z. Fisk, Phys. Rev. B **66**, 060509(R) (2002).
[53] P. J. McCarthy and H. U. Güdel, Inorg. Chem. **23**, 880 (1984).
[54] C. Bellitto, T. E. Wood, and P. Day, Inorg. Chem. **24**, 558 (1985).
[55] V. C. Long, J. L. Musfeldt, T. Schmiedel, A. Revcolevschi, and G. Dhalenne, Phys. Rev. B **56**, R14 263 (1997).
[56] A. B. Sushkov, J. L. Musfeldt, X. Wei, S. A. Crooker, J. Jegoudez, and A. Revcolevschi, Phys. Rev. B **66**, 054439 (2002).
[57] S. Zvyagin, in *Frontiers in Spectroscopy of Emergent Materials*, edited by E. C. Faulgues, D. L. Perry, and A. V. Yeremenko (Kluwer Academic, Dordrecht, 2004).
[58] H. Kishida, H. Matsuzaki, H. Okamoto, T. Manabe, M. Yamashita, Y. Taguchi, and Y. Tokura, Nature (London) **405**, 929 (2000).
[59] M. Ulutagay-Kartin, S.-J. Hwu, and J. A. Clayhold, Inorg. Chem. **42**, 2405 (2003).
[60] H. W. Eng, P. W. Barnes, B. M. Auer, and P. M. Woodward, J. Solid State Chem. **175**, 94 (2003).
[61] H. Mizoguchi, H. W. Eng, and P. M. Woodward, Inorg. Chem. **43**, 1667 (2004).
[62] J. D. Woodward, J. Choi, J. L. Musfeldt, J. T. Haraldsen, M. Apostu, R. Suryanarayanan, and A. Revcolevschi, Phys. Rev. B **69**, 104415 (2004).
[63] R. D. Willett, C. Galeriu, C. P. Landee, M. M. Turnbull, and B. Twamley, Inorg. Chem. **43**, 3804 (2004).
[64] A. W. Garrett, S. E. Nagler, T. Barnes, and B. C. Sales, Phys. Rev. B **55**, 3631 (1997).
[65] Unlike measurements of bulk properties, inelastic neuton scattering directly measures the dispersion relations of the individual magnetic excitations that allow analysis of the interactions between ions assumed in a model magnetic Hamiltonian.
[66] M.-H. Whangbo, H.-J. Koo, and D. Dai, Solid State Chem. **176**, 417 (2003).
[67] The large crystal face of $(CPA)_2CuBr_4$ corresponds to the *ab* plane (the crystallographic plane of the ladderlike arrays). However, the irregularly shaped faces and edges do not permit a visual identification of the *a* and *b* directions. Despite the orthorhombic symmetry of $(CPA)_2CuBr_4$, the in-plane optical axes are also not typically aligned with the edges of the crystals.
[68] Surface quality concerns precluded variable temperature spectroscopies below 80 K. Crystal surfaces degraded under high vacuum conditions (as well as modest vacuums for periods of 15 min or more) within the cryostat, required for base temperature measurements. Therefore, we used a ~250 Torr vacuum along with extensive helium gas backfilling of the cryostat to carry out these experiments.
[69] F. Wooten, *Optical Properties of Solids* (Academic, New York, 1972).
[70] The high frequency data were extrapolated as $\omega^{-2}$ to simulate the approach to free-electron response. The low frequency reflectance was extrapolated as a constant, as appropriate for a semiconductor.
[71] M. J. Frisch *et al.*, GAUSSIAN 98 (Revision A.9), Gaussian, Inc., Pittsburgh, PA, 1998.
[72] A. D. Becke, J. Chem. Phys. **98**, 5648 (1993); C. Lee, W. Yang, and R. G. Parr, Phys. Rev. B **37**, 785 (1988).
[73] Our calculations were carried out by employing the SAMOA (Structure and Molecular Orbital Analyzer) program package (D. Dai, J. Ren, W. Liang, and M.-H. Whangbo, http://primec.ncsu.edu/, 2002).
[74] For many crystalline samples of the title compound, the principal axes of the dielectric tensor do not perfectly correspond with the unit cell axes in the *ab*-plane despite the orthorhombic symmetry of the crystal. Nevertheless, the two optical axes are mostly along the *a* and *b* directions, corresponding to a response primarily from the bromide-bromide bridge pairs and chains, respectively.
[75] The insets of Fig. 1 show close-up views of the vibrational features at 300 K. Note the presence of the Cu-Br stretching mode at 27.5 meV (227 $cm^{-1}$), consistent with copper-halide stretching observed in similar materials (Refs. 76–78). Vibrational modes associated with the organic cation are observed in the middle infrared region.
[76] V. Stefov and B. Šoptrajanov, Vib. Spectrosc. **19**, 431 (1999).
[77] G. Marcotrigiano, L. Menabue, G. C. Pellacani, and M. Saladini, Inorg. Chim. Acta **34**, 43 (1979).
[78] D. X. West, T. J. Parsons, and R. K. Bunting, Inorg. Chim. Acta **84**, 7 (1984).
[79] $H_{c2}$ is easily distinguished in the bulk magnetization; $H_{c1}$ is not. The lower critical field was calculated to be 2 T and is consistent with that extracted from the analysis of the derivative of the magnetization in Fig. 6 (Ref. 63).
[80] D. C. Cabra and M. D. Grynberg, Phys. Rev. B **62**, 337 (2000).
[81] D. C. Cabra, A. Honecker, and P. Pujol, Eur. Phys. J. B **13**, 55 (2000).
[82] D. C. Cabra, A. Honecker, and P. Pujol, Phys. Rev. B **58**, 6241 (1998).
[83] K. Tandon, S. Lal, S. K. Pati, S. Ramasesha, and D. Sen, Phys. Rev. B **59**, 396 (1999).
[84] A. Filippetti and N. A. Hill, Phys. Rev. Lett. **85**, 5166 (2000).
[85] B. M. Suleiman and A. Lunden, J. Phys.: Condens. Matter **15**, 6911 (2003).
[86] M. Witschas, H. Eckert, H. Freiheit, A. Putnis, G. Korus, and M. Jansen, J. Phys. Chem. A **105**, 6808 (2001).